Latin American Journal of Aquatic Research, 51(2): 218-237, 2023
DOI: 10.3856/vol51-issue2-fulltext-2988

Research Article

Evaluation of the taxonomic composition of phytoplankton using microscopy and CHEMTAX in Todos Santos Bay (Baja California, México) during 2017-2018

Yessica Lizbeth Ramírez-Altamirano[1], Adriana González-Silvera[2] Jorge López-Calderón[2] & Eduardo Santamaria-del-Angel[2]
[1]Programa de Maestría en Ciencias en Oceanografía Costera, Facultad de Ciencias Marinas Universidad Autónoma de Baja California, Ensenada, BC, México
[2]Facultad de Ciencias Marinas, Universidad Autónoma de Baja California, Ensenada, BC, México
Corresponding author: Adriana González-Silvera (adriana.gonzalez@uabc.edu.mx)

ABSTRACT. This study analyzes the spatial and temporal variability of phytoplankton biomass and taxonomic composition in the surface waters of Todos Santos Bay, a semi-enclosed bay within the upwelling zone of the Baja California peninsula (México). Two methodological approaches (microscopy and chemotaxonomy [CHEMTAX]) were used to describe the variability of some genera and species (observed under the microscope) and the importance of those groups that cannot be observed microscopically. Phytoplankton biomarker pigments were measured with high-resolution liquid chromatography and used as input to run the CHEMTAX software to determine the contribution of the main phytoplankton groups to chlorophyll-*a* (Chl-*a*). The microscopic analyses showed that diatoms and dinoflagellates comprised 65 and 33% of the total cells, respectively. Dinoflagellates were most abundant in the inner bay and during cold months; the most frequent and abundant genera were *Tripos*, *Protoperidinium*, and *Prorocentrum*. Among diatoms, the most frequent genera were *Cylindrotheca*, *Guinardia*, *Navicula*, *Pseudo-nitzschia*, and *Chaetoceros*. CHEMTAX indicated that, together with diatoms, the flagellates prymnesiophytes and chlorophytes contributed a median of 80% to Chl-*a*, with chlorophytes as the most important group (29.9%). The high contribution of these flagellates suggests that they are represented by small-sized cells not visible by the light microscopy used. However, CHEMTAX largely underestimated the contribution of dinoflagellates (due to the presence of many mixotrophic species). Hence, our results emphasize the importance of using both techniques for a more detailed evaluation of the taxonomic composition of phytoplankton in this and other coastal regions.

Keywords: phytoplankton; pigments; CHEMTAX; coastal waters; temporal variability

INTRODUCTION

Phytoplankton is the primary producer in aquatic ecosystems and plays multiple ecological functions, including its role as the base of the pelagic trophic web (Falkowski et al. 1997). In turn, its size distribution is a central biological factor that determines the direction and magnitude of energy and carbon flows in the oceanic trophic web (Chisholm 1992, Finkel et al. 2010), thus affecting the productivity of marine ecosystems. Given its importance, studying its abundance and taxonomic diversity is deemed essential.

The study of the taxonomic composition of phytoplankton is traditionally based on using an inverted light microscope to visualize and quantify phytoplankton cells (Utermöhl 1958). This technique allows observing and determining certain morphological traits of a given species, such as cell size and shape, the arrangement of cells in colonies and chains, and its association with other phytoplanktonic species.

Corresponding editor: José Luis Iriarte

However, small cells (<10 µm) are not readily distinguished, and their abundance is underestimated when this method is used (Tester et al. 1995). Small species, which are more fragile or even morphologically similar, require approaches like epifluorescence, electron microscopy, or molecular techniques (Ajani et al. 2013). However, these determinations involve higher costs and are used to visualize particular species; additionally, the microscopy technique is time-consuming and requires expertise in identifying the different species.

For this reason, efforts have been made to develop methods that allow for a more detailed evaluation of phytoplankton groups (particularly the smaller ones). One such method is based on the knowledge of their pigments (Jeffrey et al. 1997). Chlorophyll-*a* (Chl-*a*) is the universal photosynthetic pigment in all plant species worldwide and is a proxy for phytoplanktonic biomass. The only exception is the cyanobacteria *Prochlorococcus* (which contains divinyl chlorophyll-*a*, or DVChl-*a*). However, phytoplankton contains other pigments; some are unique to certain algal groups, while others are shared between some phytoplanktonic groups (Table 1). Wright (1996) developed an approximation to estimate phytoplanktonic groups in a water sample based on detecting biomarker pigments. This approach is called chemotaxonomy and has recently contributed to a better understanding of the distribution and composition of oceanic and coastal phytoplankton populations, especially the smaller cells undetectable under the light microscope (Jeffrey et al. 2011, Araujo et al. 2016, among others). Chemotaxonomy is done using the CHEMical TAXonomy software (CHEMTAX), which calculates the percentage of each algal class in a sample from the concentration of diagnostic pigments determined by high-performance liquid chromatography (HPLC) (Mackey et al. 1996). This software optimizes the contribution of each phytoplankton group regarding Chl-*a* based on a factorial analysis and the steepest descent algorithm, estimating the best fit of the proportions of the pigments measured by HPLC.

Todos Santos Bay is located on the northwest coast of Baja California, Mexico, between 31°40'-31°56'N and 116°36'-116°50'W. A semi-enclosed coastal water body whose oceanographic variability is strongly linked to the influence of the California Current System (CCS) (Mateos et al. 2009), its bathymetry, the configuration of the coastline, and the effect of local and remote processes generated by wind, tides, and other forcing agents (Flores-Vidal et al. 2018). The CCS is characterized by a year-round southward water flow dominated by the California Current, which carries cold, low-salinity waters near the bay (Durazo 2015). Underneath, the California Countercurrent flows northward, transporting saline water with high nutrient concentrations. These can be carried to the surface during upwelling events and affect the interior of the bay by fertilizing surface waters and promoting phytoplankton blooms (García-Mendoza et al. 2009). The bay is also influenced by wastewater discharges (domestic and industrial) and agricultural runoff (Tanahara et al. 2021). Its economy depends primarily on maritime trade and tourism. Besides, harmful algal blooms (HABs) are regularly recorded in the region, highly relevant to the regional economy and ecosystem health (Medina-Elizalde et al. 2016). Finally, regional-scale events have been recorded in the bay, such as the recent Pacific warm anomaly (the Blob), which led to a significant reduction in phytoplankton biomass (Delgadillo-Hinojosa et al. 2020) and abundance (Jiménez-Herrera 2017), particularly affecting the development of bivalve mollusk cultures. Therefore, studying phytoplankton dynamics and the changes in its taxonomic composition is paramount since its variability influences the entire ecosystem and human societies.

This paper reports the results of a study conducted between 2017 and 2018 that evaluated the spatial-temporal variability of the phytoplankton taxonomic composition using light microscopy and chemotaxonomy, aiming to contribute to a) the knowledge of the spatial-temporal variability of phytoplankton groups in the bay, and b) the usefulness of using chemotaxonomy together with traditional microscopy for the description of small-sized groups.

MATERIALS AND METHODS

Eight cruises were conducted between February 2017 and October 2018, recording surface data from six stations (Fig. 1). These were classified as a representative of the outer or oceanic zone (B1, B2, and B3) and the inner or coastal zone (B4, B5, and B6) of the bay. During the sampling on June 2, 2017, the dinoflagellate *Lingulodinium polyedra* bloomed. The data from this cruise is treated separately to avoid skewing the overall trends observed.

Surface water from each station was collected with a bucket. Amber high-density polyethylene (Nalgene) bottles containing 2.5 mL of alkaline Lugol's solution (sodium acetate) were filled with 250 mL of water sample to preserve cells (Throndsen 1978) for subsequent identification and quantification of phyto-

Table 1. Distribution of biomarker pigments according to phytoplankton groups (based on Jeffrey et al. 1997).

Pigment	Abbreviation	Group
Chlorophyll-*a*	Chl-*a*	All groups (except *Prochlorococcus*)
Monovinyl chlorophyll-*b*	Chl-*b*	Chlorophytes, Prasinophytes, Euglenophytes
Fucoxanthin	Fuco	Bacillariophytes, Prymnesiophytes
Peridinin	Peri	Dinophytes
19'-Butanoyloxyfucoxanthin	19´-But	Chrysophytes, Prymnesiophytes
19'-Hexanoyloxyfucoxanthin	19´-Hex	Prymnesiophytes
Alloxanthin	Allo	Cryptophytes
Zeaxanthin	Zea	Cyanobacteria, *Prochlorococcus*, Chlorophytes
Lutein	Lut	Chlorophytes, Prasinophytes
Violaxanthin	Viola	Chlorophytes, Prasinophytes

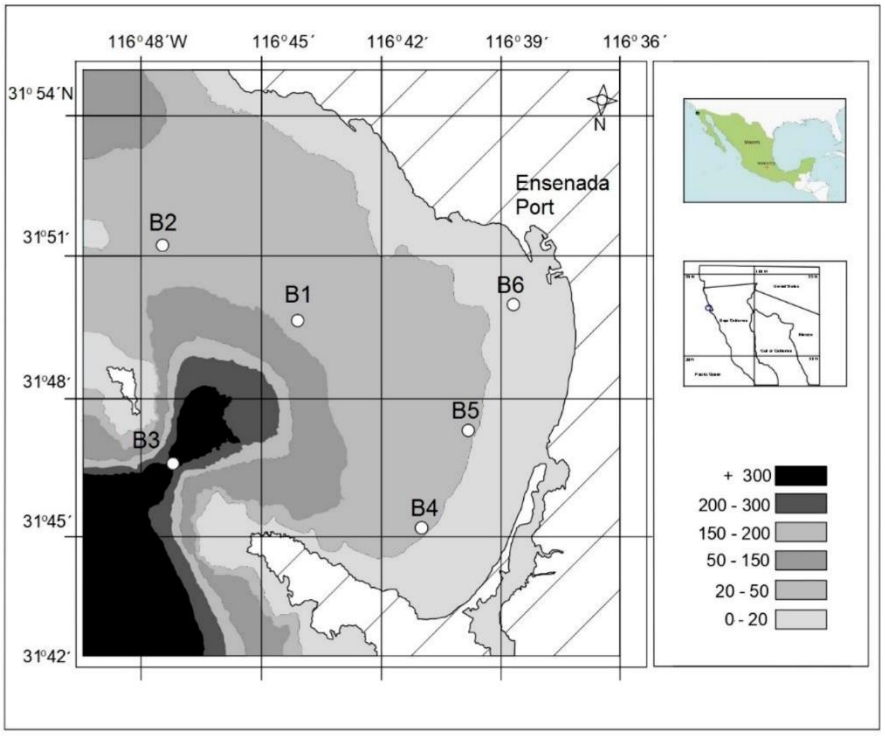

Figure 1. Map of the study area where sampling stations are marked. Colors indicate the local bathymetry (color palette in meters).

plankton under the microscope. The remaining water was reserved in 8 L amber high-density polyethylene (Nalgene) bottles, which prevent light penetration; samples were transported fresh to the laboratory.

In the laboratory, between 1 and 2 L of water from each station were filtered using positive-pressure filtration through Whatman GF/F glass fiber filters (25 mm diameter), which were then stored in aluminum foil sachets in liquid nitrogen for subsequent measurement of pigment concentrations.

Satellite images and upwelling index

Multisensor composites were built following the criteria of Kahru et al. (2012, 2015). Monthly multisensor images (MODIS/Aqua, MODIS/Terra, and VIIRS) of sea surface temperature (SST) were processed between January 2017 and December 2018 at 1 km spatial resolution using SeaDAS V7.1 to assess the seasonal variability in the study area and locate the sampling days within the two years of work. The SST time series was extracted for stations B2 and B5, which

are deemed representative of the outer and inner areas of the bay, respectively.

The regional effect of coastal upwelling events was assessed by obtaining monthly upwelling index averages for the locality 30°N-119°W (https://oceanwatch.pfeg.noaa.gov/products/PFELData/upwell/monthly/upindex.mon).

Phytoplankton identification and abundance

The Uthermöl (1958) method estimated the abundance of cells using a Zeiss IM phase contrast inverted microscope. Sedimentation columns of different volumes were used. We used 100 and 50 mL columns for oceanic samples and 50 and 25 mL columns for coastal samples. Phytoplankton cells were counted and identified to genus level and, in some cases, species level; abundance was recorded in cells L^{-1}. Identification was based on the guides of Throndsen (1993), Tomas (1997), Meave del Castillo (1999), Góngora-González (2003), Dimar-CIOH (2011), Almazán-Becerril et al. (2016), and Morales-Pulido & Aké-Castillo (2019). Also, information and references from Guiry & Guiry (2022) in AlgaeBase (https://www.algaebase.org/) were used.

The smaller samples (50 and 25 mL) were first observed at 400x and 200x, followed by the 100 and 50 mL samples. However, previously observed genera or species were not counted in the last samples, aiming to identify the less abundant genera.

HPLC pigment analysis

Pigments were analyzed using the method of Van Heukelem & Thomas (2001), modified by Thomas (2012), with an Agilent 1260 HPLC apparatus. The pigments were separated by a Zorbax Eclipse XDB C8 column (4.6' 150 mm, 3.5 pore diameter) at 60°C, using three solvents (A, B, and C). Solvent A: 70% methanol: 30% 0.028 M tetrabutyl ammonium acetate (pH 6.5); solvent B: 100% methanol at a 1 mL min^{-1} flow rate; solvent C: 100% acetone. The pigments identified in this study are shown (Table 1).

Internal standards were obtained from the DHI Water and Environment (Hørsholm, Denmark) for each pigment. The HPLC was calibrated with these standards, with concentrations measured by an Agilent Cary 100 spectrophotometer using the absorption coefficients reported in the literature (Hooker et al. 2009) or provided by DHI. DVChl-*a*, a diagnostic pigment for the cyanobacteria genus *Prochlorococcus*, was not detected.

CHEMTAX

The relative abundance of microalgae classes contributing to total Chla-*a* biomass was calculated using the CHEMTAX version 1.95 software (Mackey et al. 1996). The proportions of the indicator pigments of the main phytoplankton classes (diatoms, dinoflagellates, cyanobacteria, cryptophytes, chrysophytes, chlorophytes, and prymnesiophytes), i.e. the initial matrix (Table 2), were obtained from González-Silvera et al. (2020). The pigment concentrations measured by HPLC were incorporated into CHEMTAX. The results showed a series of 64 output matrices indicating the contribution of phytoplanktonic groups to the concentration of pigments in the initial matrix. Ten percent of the matrices with the lowest root mean squared error (RMSE) were selected and averaged to obtain the final output matrix (Supplementary Material, Table S1), according to Wright et al. (2009).

RESULTS

The study period was characterized by a marked seasonality (Fig. 2), with the lowest temperatures observed from November to May and the highest from July to October. Overall, 2017 was cooler than 2018, and temperatures at station B2 (representing the oceanic stations) tend to be lower than at the inner bay area (station B5). This difference was more pronounced in June 2017, having characteristics of the cold period, when the difference in temperature between stations B2 and B5 was almost 4°C. This month, an *L. polyedra* bloom occurred due to increased upwelling intensity and a marked drop in SST at station B2 (16.6°C).

Phytoplankton taxonomic composition and biomass

The microscope analyses identified three major groups: diatoms, dinoflagellates, and nanoflagellates (Table S2). In general, diatoms were the most abundant group and comprised 65% of the total cells, followed by dinoflagellates with 33%. However, this contribution changed over time and space (Figs. 3-4).

Cell abundance ranged from 0.79 to 38.4×10^3 cells L^{-1} (Figs. 3-4) without a well-defined temporal pattern. Oceanic stations (Fig. 3) showed a positive trend in phytoplankton abundance toward the warm months, while coastal stations (Fig. 4) displayed the highest abundances, although with wider variations. In oceanic stations, the highest abundance was observed at station B2 (June 2018), especially due to *Ceratium tripos var. divaricatum* (9.26×10^3 cells L^{-1}) high abundance. In

Table 2. Initial pigment ratios used in the CHEMTAX analysis. Pigment abbreviations are indicated in Table 1.

Grup/Pigment	Chl-*b*	19´-But	19´-Hex	Allo	Fuco	Peri	Zea	Lut	Chl c_3
Diatoms	0	0	0	0	0.62	0	0	0	0
Dinoflagellates	0	0	0	0	0	0.56	0	0	0
Prymnesiophytes	0	0.05	0.42	0	0.27	0	0	0	0.174
Chlorophytes	0.32	0	0	0	0	0	0.03	0.17	0
Cryptophytes	0	0	0	0.38	0	0	0	0	0
Cyanobacteria	0	0	0	0	0	0	0.64	0	0
Chrysophytes	0	0.35	0	0	0	0	0	0	0.23

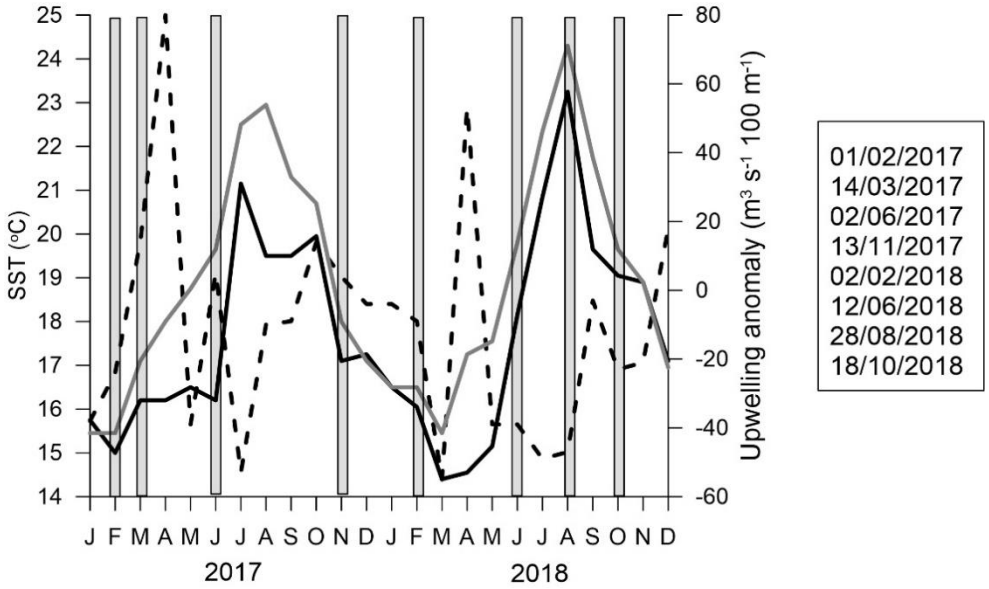

Figure 2. Time series of sea surface temperature (SST) for station B2 (solid black line) and station B5 (solid gray line) and of the upwelling index anomaly (dotted line, right axis). Sampling dates (day/month/year) are shown in the table. Vertical bars indicate the month of each sampling.

coastal stations, the highest abundance occurred in October 2018 (stations B4 and B5), dominated by the diatom *Hemiaulus hauckii*, with abundances of up to 33×10^3 cells L^{-1}.

A total of 127 genera were identified. The genera and species identified and an indication of their presence or absence for each sampling date are listed in the Supplementary Material (Table S2). Among diatoms, the genera or species most frequently observed were *Cylindrotheca closterium*, *Guinardia striata*, *Navicula* sp., *Pseudo-nitzschia* sp., and several species of *Chaetoceros* sp. *Hemiaulus hauckii* was abundant only in the last two sampling events (August and October 2018). Among the dinoflagellates, *Tripos* spp. (*T. furca* and *T. fusus*), *Protoperidinium* sp. and *Prorocentrum gracile* were observed in all sampling dates, although not always in all stations. The genus *Cochlodinium* sp. occurred at all stations in the last three samplings (June, August, and October 2018). On the other hand, *Lingulodinium polyedra* was observed at all stations but only in three months (June 2017, February, and June 2018).

The temporal variation in the abundance of the most frequent genera or species is shown (Figs. 3-4). The first two months of sampling (February and March 2017) showed an almost total prevalence of dinoflagellates at all stations, especially of the genera *Tripos* and *Prorocentrum*. However, abundances were less than 2×10^3 cells L^{-1} at stations B1 (Fig. 3), B4, B5, and B6 (Fig. 4) but exceeded 10×10^3 cells L^{-1} at stations B2 (Fig. 3c) and B3 (Fig. 3e). These were the highest dinoflagellate abundances recorded over the entire study period except the *L. polyedra* bloom (June 2017). It is worth noting that *L. polyedra* was observed over

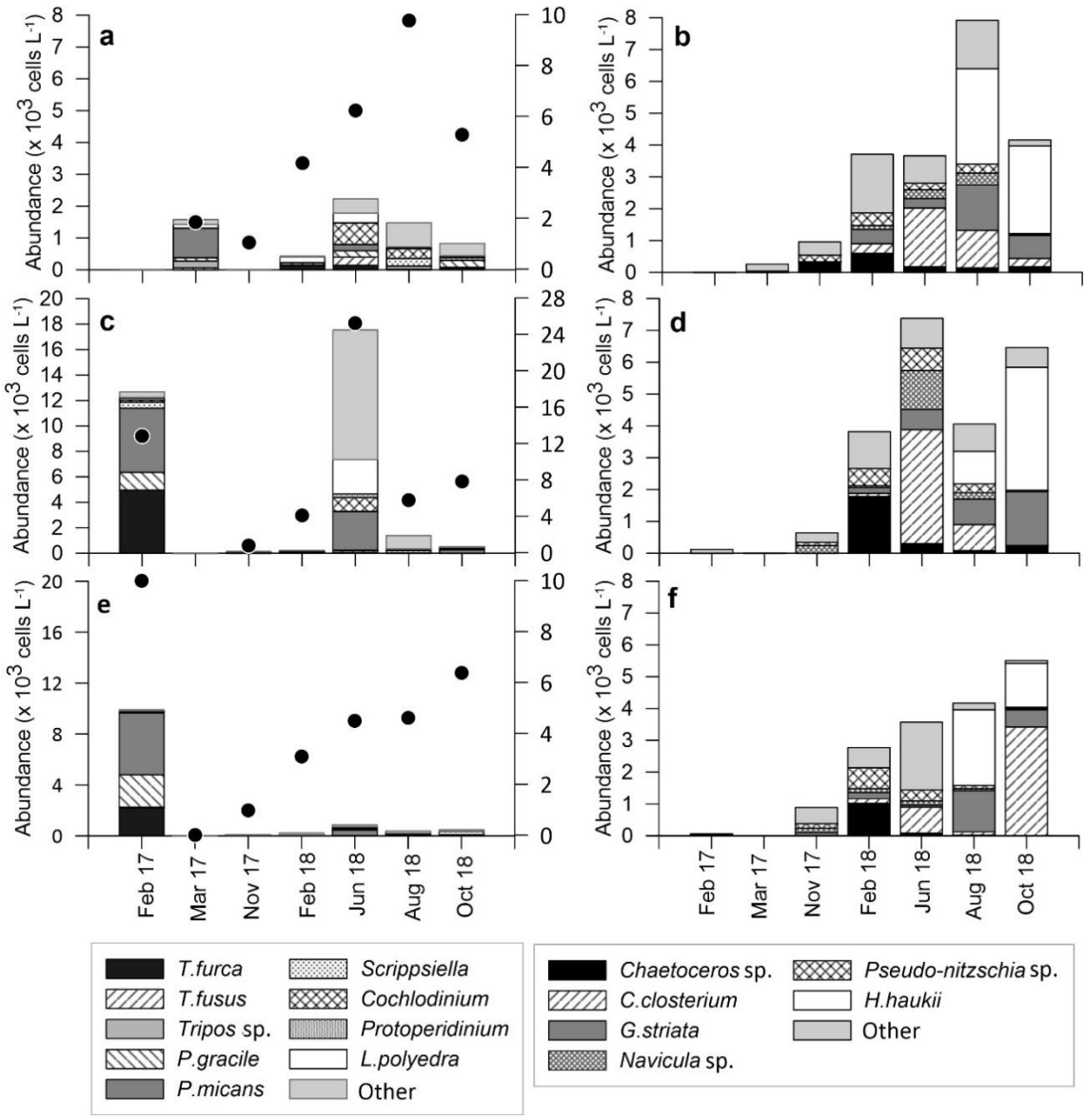

Figure 3. Cell abundance ($\times 10^3$ cells L^{-1}) of the major genera or species of dinoflagellates (a-c-e) and diatoms (b-d-f) identified under the microscope for stations B1 (a-b), B2 (c-d), and B3 (e-f). In the graphs on the left, dots represent total abundance ($\times 10^3$ cells L^{-1}, right axis in a, c and e).

almost the whole study period and at all stations, although not in very high abundances (between 0.04×10^3 and 2.68×10^3 cells L^{-1}). Overall, the abundance of dinoflagellates was higher at coastal stations (except for February 2017 in the oceanic B2 and B3), while diatom abundances were more comparable (except for the higher values in October 2018 in B4 and B5).

Diatom abundance generally showed the same increasing trend over time, most evident at the oceanic stations (Fig. 3). Coastal stations (Fig. 4) displayed greater variability in diatom abundance and diversity. The genus *Chaetoceros* occurred in almost all samplings and stations, being more abundant at coastal stations, reaching values of 2×10^3 cells L^{-1} (station B6) in November 2017 and February 2018. There was a marked increase in the abundance of *H. hauckii* in the last two months of sampling when it reached 33×10^3 cells L^{-1} (station B4). On the other hand, the peak in abundance of diatoms at oceanic stations occurred in B1 and B2, dominated by *C. closterium* and *G. striata*.

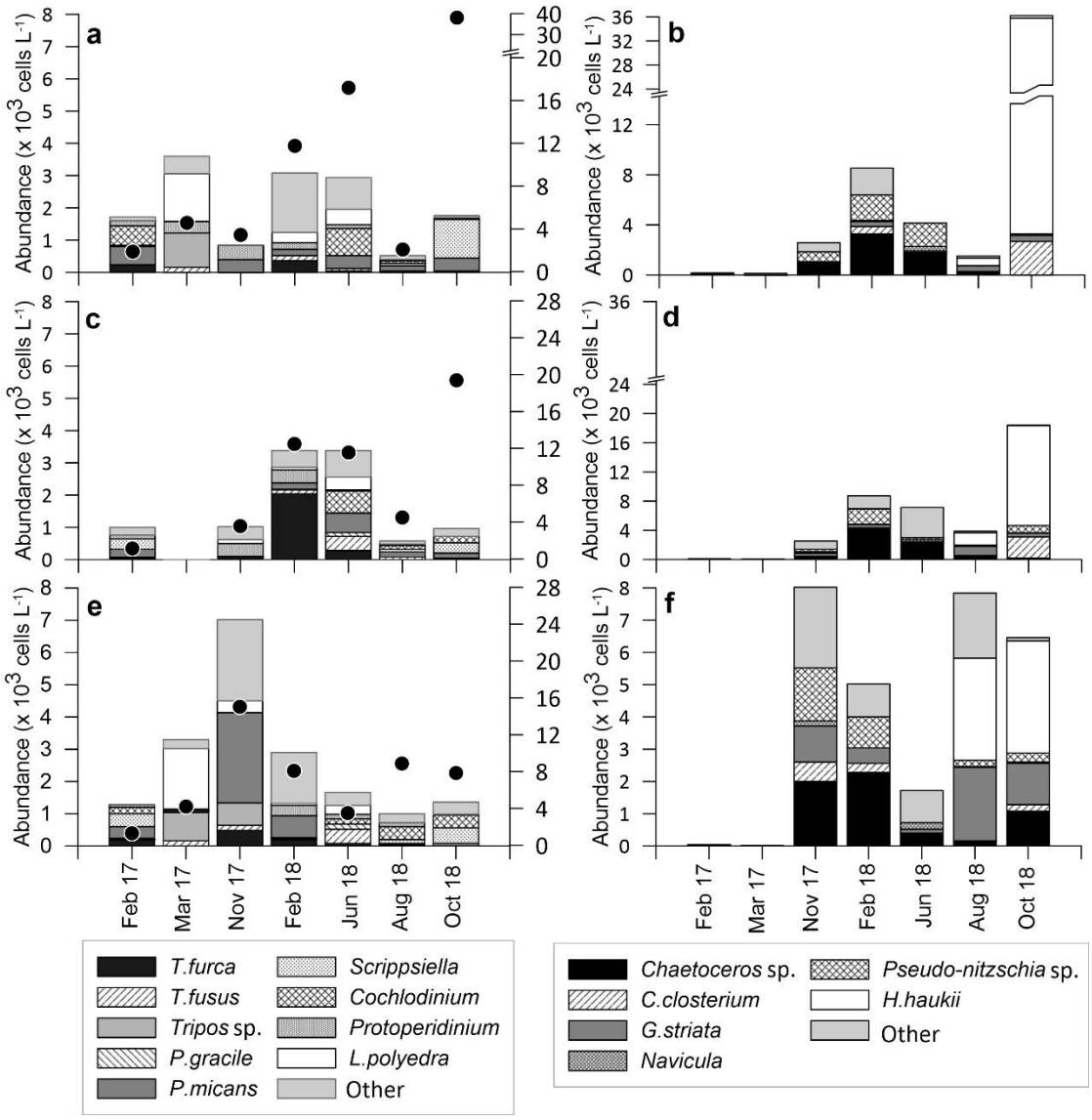

Figure 4. Cell abundance ($\times 10^3$ cells L^{-1}) of the major genera or species of dinoflagellates (a,c,e) and diatoms (b-d-f), identified under the microscope for stations B4 (a-b), B5 (c-d), and B6 (e-f). In the graphs on the left, dots represent total abundance ($\times 10^3$ cells L^{-1}, right axis in a, c and e).

Pigments and chemotaxonomy

Chl-*a* concentrations varied between 0.11 and 3.46 mg m^{-3} with a median of 0.57 mg m^{-3} (Fig. 5, Table 3), with no clear temporal pattern. In oceanic stations (Fig. 5a-c), Chl-*a* concentration was generally less than 0.8 mg m^{-3}; it only exceeded 1 mg m^{-3} in February 2017 (B2 and B3), June 2018, and October 2018 (B2). On the other hand, in the three coastal stations (Fig. 5e-f), the highest Chl-*a* concentrations were recorded at station B6, with a peak in November 2017.

The determination of phytoplanktonic groups by CHEMTAX showed that, in addition to the diatoms and dinoflagellates observed under the microscope, flagellates such as prymnesiophytes, chlorophytes, and cryptophytes were found in all stations (Fig. 5). Table 3 shows the ranges of variation and the median of the phytoplankton groups contributing to total Chl-*a*. Regarding the median, diatoms, prymnesiophytes, and chlorophytes comprised 80% of the community contribution to Chl-*a*. The highest contribution was by chlorophytes (29.9%), while cyanobacteria had the lowest contribution (0.7%). No well-defined temporal or spatial trends in the distribution of groups were observed; however, diatoms tend to display higher contributions to Chl-*a* in coastal stations.

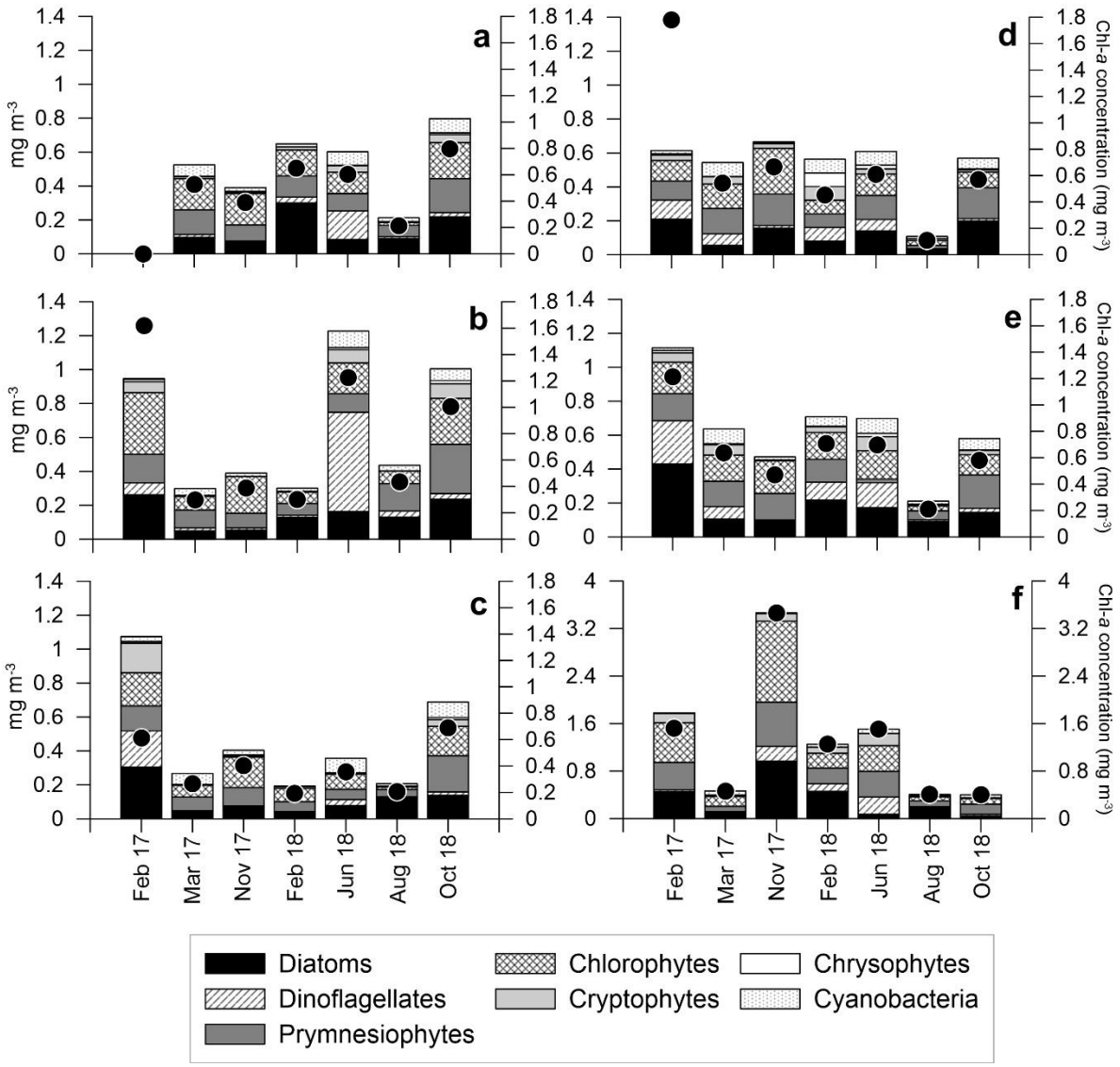

Figure 5. Contribution of algal groups to Chl-*a* determined by CHEMTAX (left axis, mg m^{-3}) and Chl-*a* concentration (right axis, mg m^{-3}) for stations a) B1, b) B2, c) B3, d) B4, e) B5, and f) B6.

Table 3. Ranges of variation (minimum and maximum) and median concentration of algal groups to chlorophyll-*a* (Chl-*a*, mg m^{-3}). The relative contribution of each group to the community, expressed in percentage, is indicated in parentheses; groups with a contribution greater than 20% are highlighted in bold.

	Min	Max	Median		Min	Max	Median
Diatoms	0.03	0.969	0.128 (**24.8%**)	Cryptophytes	0	0.204	0.024 (4.6%)
Dinoflagellates	0	0.585	0.031 (5.9%)	Chrysophytes	0	0.097	0.041 (7.9%)
Prymnesiophytes	0.02	0.743	0.135 (**26.1%**)	Cyanobacteria	0	0.08	0.004 (0.7%)
Chlorophytes	0.016	1.362	0.154 (**29.9%**)				

Lingulodinium polyedra bloom

On June 2, 2017, an intense bloom of the dinoflagellate *L. polyedra* was observed, characterized by abundances reaching up to 145×10^3 cells L^{-1} and 11.3 mg m^{-3} Chl-*a* at station B6 (Fig. 6). Although this bloom was most evident at this station, *L. polyedra* was observed in all stations, with a minimum of 4×10^3 cells L^{-1} at station B2.

The most abundant diagnostic pigment was peridinin (characteristic of dinoflagellates), which is reflected in the results of the chemotaxonomic analysis (Fig. 6b). The high contribution of dinoflagellates to Chl-*a* at stations B4 and B6 was estimated, consistent with our findings under the microscope. However, a high contribution by prymnesiophytes to Chl-*a* was also determined, especially at the three coastal stations. On the other hand, oceanic stations showed an increased contribution of cyanobacteria and chlorophytes to Chl-*a*. Notably, no diatoms were estimated by CHEMTAX at station B6, which is consistent with the microscope observations (Fig. 6a).

DISCUSSION

The taxonomic composition and biomass of phytoplankton in Todos Santos Bay were characterized by a seasonal cycle associated with the dynamics of coastal upwelling events, which intensify during the spring and summer when larger diatoms grow as a result of the increased input of nutrients. Late summer and autumn have been associated with an increase in the abundance of flagellates and dinoflagellates; finally, in winter, biomass and diversity drop to minimum levels (García-Mendoza et al. 2009, Almazán-Becerril et al. 2016). The trends found here are consistent with previous observations. That is, considering the first four samplings as characteristic of the cold season and the last three of the warm season, an increase in cell abundances from the cold to the warm months was evident, as well as the shift in the dominance of dinoflagellates to diatoms. The highest cell abundance in oceanic stations occurred in June 2018 at station B2 (Fig. 3c-d), the sampling station closest to the adjacent oceanic zone most affected by nutrient input associated with upwelling events. Evidently, changes in upwelling intensity affect the seasonal variability pattern, observed by comparing June 2018 with June 2017. In 2017, the bloom of the dinoflagellate *L. polyedra* occurred (Fig. 6), coinciding with positive anomalies in the upwelling index, low temperatures (16.6°C) in the outer zone of the bay, and high temperatures (18.8°C) in the inner zone (Fig. 2). Contrasting characteristics were observed in 2018, with lower cell abundances and a greater prevalence of diatoms (especially *C. closterium*), particularly at station B2.

It is important to analyze not only temporal variability - which in this study was limited by the varying sampling frequency - but also spatial variability. That is, the trends of increasing abundance toward the warm months are clearer in oceanic stations (B1-B3), while the coastal stations (B4-B5) displayed a greater variability (Figs. 3-4). Several studies have reported differences in phytoplankton abundance and biomass between the outer and inner bay (Delgadillo-Hinojosa et al. 2015, 2020, Jiménez-Herrera 2017, Oliva-Méndez et al. 2018), which has been associated with the fact that the outer areas are affected to a greater extent by the dynamics of the adjacent oceanic zone and, therefore, by the seasonal cycle of upwellings and interannual processes. On the other hand, in shallower zones, the circulation processes associated with the wind and coastal morphology impose differences in the dynamics of biochemical processes (Delgadillo-Hinojosa et al. 2015). Our results showed cooler waters in outer areas and warmer in inner zones, as Olivas-Méndez et al. (2018) described. Jiménez-Herrera (2017), in a study conducted between August 2014 and December 2015, observed that the inner zone of the bay is characterized by higher cell abundances than the outer zone, although with important seasonal changes. In the present study, these differences were more marked for dinoflagellates than for diatoms; the former tend to be more abundant near the coast (Figs. 3-4).

Concerning the dominant genera and species, the most abundant genus was *Tripos* (especially *T. furca* and *T. fusus*). Both species were present in almost all the samplings, consistent with previous studies (Peña-Manjarrez et al. 2005, Almazán-Becerril et al. 2016, Fimbres-Martínez 2019). *T. furca* is very common in BTS and can reach very high abundances; it is reported as a potentially harmful species since its blooms have been related to the high mortality of tuna fish and some invertebrates in the bay (Orellana-Cepeda et al. 2004). Among the genera and species most frequently observed in this study (Figs. 4-5), *P. micans*, *Scrippsiela* sp., and *Cochlodinium* sp., in addition to *L. polyedra*, have been reported as forming harmful algal blooms, some associated with the production of toxins (Cortés-Lara et al. 2004, Peña-Manjarrez et al. 2005, 2009, Medina-Elizalde et al. 2016). In Todos Santos Bay, *Cochlodinium* (probably *C. fulvescens*), an ichthyotoxic species, was first recorded between November and December 2016, associated with signi-

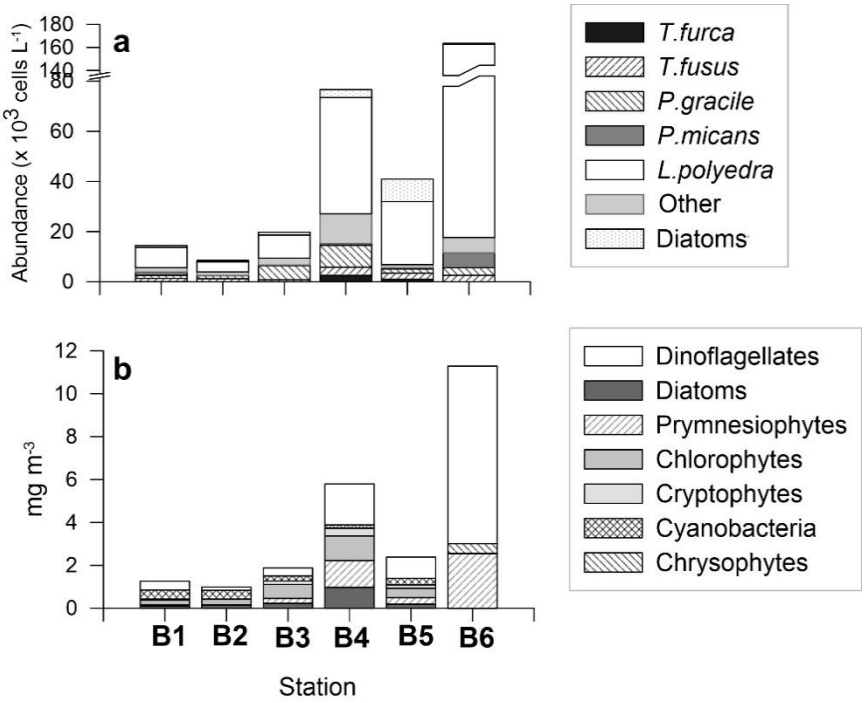

Figure 6. a) Cell abundance ($\times 10^3$ cells L^{-1}) observed under the microscope indicating the most abundant dinoflagellates, other dinoflagellates, and diatoms, and b) contribution of algal groups to Chl-*a* determined by CHEMTAX (mg m^{-3}).

ficant tuna mortality south of the bay (Fimbres-Martínez 2019). Our study period overlaps with the time window mentioned above (2016-2017) but extends to 2018, observing that the presence of *Cochlodinium* sp. was maintained, especially at coastal stations, although with abundances that did not exceed 1×10^3 cells L^{-1}. Fimbres-Martínez (2019) determined that this genus flourished due to upwellings within a temperature range of 14 to 16°C. However, in 2018, this genus was observed during the warm months (June to October), when sea surface temperatures (SST) were above 18°C, which may explain the low abundance observed during these months. Nevertheless, this species, potentially forming harmful algal blooms (with resistance cysts found in the marine sediment), remains in the bay and is potentially risky to tuna feeding activities.

Diatoms were the dominant group in the samplings performed in this study, including mainly chain-forming species such as *Chaetoceros* sp., *Pseudo-nitzschia* sp., *Cylindrotheca closterium*, *Guinardia striata*, and *Hemiaulus hauckii*. All these genera or species have been observed in the bay in previous studies (Martínez-Gaxiola et al. 2007, Almazán-Becerril et al. 2016, Jiménez-Herrera 2017, Fimbres-Martínez 2019). The presence of chain-forming species has been related to the months after the intensification of coastal upwelling, when they can even develop massive blooms (García-Mendoza et al. 2009). However, this study observed the highest diatom abundances in the months with the lowest upwelling intensity (June to October 2018). During this period, *C. closterium* was one of the species in all sampling stations, with its greatest abundance (maximum 3.6×10^3 cells L^{-1}) in oceanic stations. A study conducted between April and September 2005 (Martínez-Gaxiola et al. 2007) found that this diatom had very high abundances (1×10^6 cells L^{-1}) in a coastal area of the bay in May associated with a dinoflagellate bloom.

The phytoplankton biomass, Chl-*a*, in Todos Santos Bay and the adjacent oceanic zone, has been reported as dependent on the seasonal cycle of upwelling events, with high values in spring and low in autumn and winter (Espinosa-Carreón et al. 2001, Delgadillo-Hinojosa et al. 2015, 2020). However, this seasonal variability can be affected by interannual events such as El Niño or warm anomalies such as the Blob (Delgadillo-Hinojosa et al. 2020). During upwelling periods (April to August), surface Chl-*a* in the bay varied between 2.1 mg m^{-3} (inner zone) and 2.21 mg m^{-3} (outer zone), while during warm anomalies, these decreased to 1.03 and 0.77 mg m^{-3} (El Niño) or between 0.68 and 0.56 mg m^{-3} (the Blob), respectively (Delgadillo-Hinojosa et al. 2020). These observations show that the maximum

concentrations are recorded at the inner bay in periods of warm anomalies. In contrast, in the upwelling season, these correspond to the outer zone of the bay (i.e. due to the effect of upwelling events). In our study, Chl-*a* concentrations were commonly observed within the range associated with a warm anomaly (median of 0.57 mg m^{-3}) and with no clear relationship with upwelling intensity. In addition, the highest concentrations were also found in the coastal area of the bay. Despite the irregular frequency of our sampling, these findings seem to indicate an oligotrophic period in the bay in these two years of sampling.

Regarding the contribution of phytoplankton groups to Chl-*a* as determined from chemotaxonomy, the results of this study show the importance of prymnesiophytes and chlorophytes within the phytoplanktonic community, in addition to the diatoms observed using the traditional techniques. Together, these three groups contribute a median of 80% to Chl-*a* (Table 3). Prymnesiophytes and chlorophytes are defined as phytoflagellates (Jeffrey et al. 1997), with sizes in the ranges of nano- and picoplankton (<20 μm). In this study, chlorophytes had the greatest contribution, with a median of 29.9% of the total abundance. Almazán-Becerril et al. (2016) emphasized that, in general, flagellates are the most abundant phytoplankton group in Todos Santos Bay and recorded the presence of prymnesiophyte and chlorophyte species in both inner and outer areas of Todos Santos Bay. However, very few of these flagellates could be identified under the microscope in the present study (Table S2), and these were either very infrequent or found with very low abundances. For example, the prymnesiophyte *Phaeocystis* sp., observed in almost all stations in October 2018, had a peak abundance of 440 cells L^{-1}.

On the other hand, only one chlorophyte species, *Pyramimonas grossii*, was identified on a single occasion, also in October 2018. The high contribution of these two groups determined by chemotaxonomical analysis leads to two important conclusions: a) these groups are represented by species of size smaller than 5 μm; therefore, they cannot be detected using light microscopy, and b) the abundance and ecological role of these phytoplankton groups in the bay has been underestimated. It should be noted that a recent study in a coastal station located 10 km off Todos Santos Bay (Gonzalez-Silvera et al. 2020) determined a significant increase in pico- and nanoplankton flagellates (especially chlorophytes and prymnesiophytes) during the 2014 Blob warm event and the 2015-2016 El Niño, compared to previous years not affected by these events. In Todos Santos Bay, it remains to be clarified whether the high contribution of these groups during those years (2017 and 2018) is due to an anomalous event or because these are permanent components of the phytoplankton community.

Our results emphasize the importance of chlorophytes and prymnesiophytes in Todos Santos Bay, which could not have been quantified previously based solely on light microscopy. These groups predominate under oligotrophic conditions (Mouw et al. 2016), suggesting that these conditions may have characterized our study period.

On the other hand, our results showed the poor efficacy of chemotaxonomy in estimating the abundance of dinoflagellates because the chemotaxonomic detection of this group is based on peridinin. However, dinoflagellates also have mixotrophic or heterotrophic strategies. Hence some species lack this biomarker pigment. For example, the genus *Tripos* (particularly *T. furca*) - one of our study's most frequent and abundant genera may have autotrophic and mixotrophic strategies (Smalley & Coats 2002, Baek et al. 2011). While, during the bloom of *L. polyedra* - also a mixotrophic dinoflagellate (Jin-Jeong et al. 2005), dinoflagellate abundance determined by chemotaxonomy explained 99% of the variability in *L. polyedra* abundance determined by microscopy ($R^2 = 0.99$; n = 6) since an autotrophic process drove cell growth.

It was observed that microscopy and chemotaxonomy do not always reveal the same spatial or temporal trends in diatom abundance (Fig. 5). In a first approximation, this was assessed using a scatter plot, which revealed a poor linear relationship between the two estimates (Fig. 7).

On several occasions, chemotaxonomy revealed the presence of diatoms when they were not observed under the microscope (points on the *y*-axis in Figure 7). This is in great part because the estimation of diatoms by chemotaxonomy is based on the biomarker pigment fucoxanthin (Table 1).

However, this pigment is also present in prymnesiophytes and may explain the overestimation observed in our data. By excluding these and the other two outliers from the analysis, a clearer linear trend in the relationship between these approximations is obtained (Fig. 7b).

Finally, it must be considered that the concentration of pigments inside the cells varies according to the light to which they have been exposed, so a higher concentration of a certain marker pigment may be due to photoacclimation and does not necessarily to a larger proportion of the given group (Higgins et al. 2011).

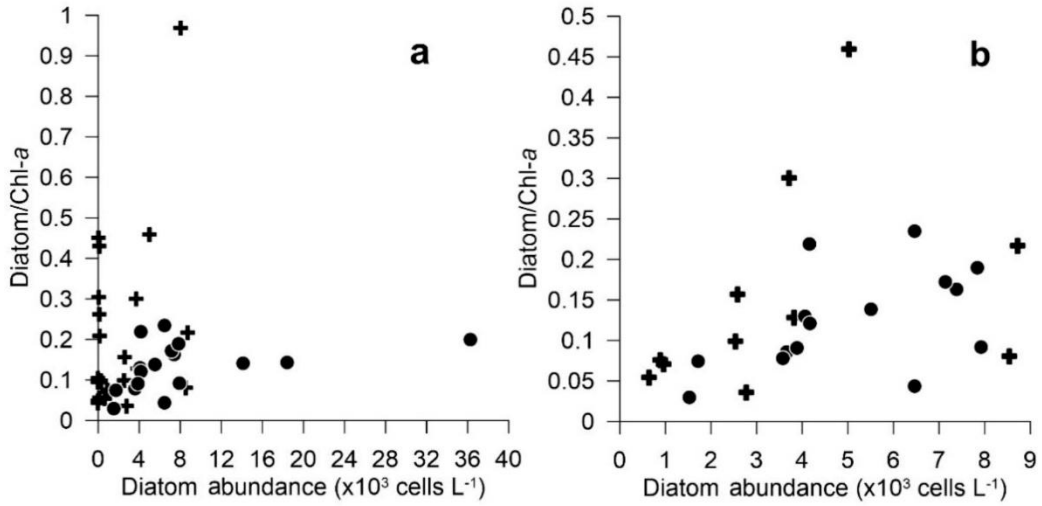

Figure 7. a) Scatter plot relating diatom abundance determined by microscopy (*x*-axis) and diatom contribution to chlorophyll-*a* determined by chemotaxonomy (*y*-axis). Circles and crosses indicate data from the warm and cold season samplings, respectively. b) Same data after outliers have been excluded (see explanation in the text).

The use of biomarker pigments to investigate the taxonomic composition of phytoplankton in ocean waters has been a valuable tool since its emergence, especially for elucidating the contribution of small-sized groups. It is especially important if it is considered the high contribution of flagellates (such as prymnesiophytes and chlorophytes) to Chl-*a* as it was determined in this study. A high contribution of flagellates and heterotrophic dinoflagellates indicates the importance of a multivorous food web, typical of ecosystems capable of recycling carbon efficiently (Stoecker et al. 2017). However, it may also indicate an inefficient carbon transfer to other trophic levels, as previously suggested for the coastal zone outside Todos Santos Bay (Linacre et al. 2012).

ACKNOWLEDGMENTS

Thanks to the Consejo Nacional de Ciencia y Tecnología (National Council of Science and Technology, CONACYT, Mexico) for the postgraduate scholarship granted to JLRA. This work was conducted with support from the CONACYT project CF-2019-1327711 and POGO and Nippon foundation (NF-POGO) through the NANO-DOAP project (https://nf-pogo-alumni.org/projects/global/). María Elena Sánchez-Salazar translated the manuscript into English. We gratefully acknowledge anonymous reviewers' comments and suggestions that helped improve this paper.

REFERENCES

Ajani, P., Murray, S., Hallegraeff, G., Brett, S. & Armand, L. 2013. First reports of *Pseudo-nitzschia micropora* and *P. hasleana* (Bacillariophyceae) from the Southern Hemisphere: Morphological, molecular and toxicological characterization. Phycology Research, 61: 237-248. doi: 10.1111/pre.12020

Almazán-Becerril, A., Aké-Castillo, J.A., García-Mendoza, E., Sánchez-Bravo, Y.A., Escobar-Morales, S. & Valadez-Cruz, F. 2016. Catálogo de microalgas de Bahía de Todos Santos, Baja California, México. CICESE, Ensenada.

Araujo, V.M.L., Borges, M.C.R., Tavano, V.M., Eiras, G.C.A. & O´Neil, B.M. 2016. Contrasting patterns of phytoplankton pigments and chemotaxonomic groups along 30°S in the subropical South Atlantic Ocean. Deep-Sea Research I, 120: 112-121. doi: 10.1016/j.dsr.2016.12.004

Baek, S.H., Shin, H.H., Choi, H.W., Shimode, S., Hwang, O.M., Shin, K. & Kim, Y.O. 2011. Ecological behavior of the dinoflagellate *Ceratium furca* in Jangmok harbor of Jinhae Bay, Korea. Journal of Plankton Research, 33: 1842-1846. doi: 10.1093/plankt/fbr075

Chisholm, S.W. 1992. Phytoplankton size. In: Falkowski, P.G. & Woodhead, A.D. (Eds.). Primary productivity and biogeochemical cycles in the sea. Plenum Press, New York, pp. 213-237.

Cortés-Lara, M., Cortés-Altamirano, R. & Sierra-Beltrán, A. 2004. Presencia de *Cochlodinium catenatum* (Gymnodiniales: Gymnodiniaceae) en mareas rojas de Bahía de Banderas, Pacífico mexicano. 2004. Revista de Biología Tropical, 52: 35-49.

Delgadillo-Hinojosa, F., Camacho-Ibar, V., Huerta-Díaz, M.A., Torres-Delgado, V., Pérez-Brunius, P., Lares, M.L., et al. 2015. Seasonal behavior of dissolved cadmium and Cd/PO_4 ratio in Todos Santos Bay: a retention site of upwelled waters in the Baja California peninsula, Mexico. Marine Chemistry, 168: 37-48. doi: 10.1016/j.marchem.2014.10.010

Delgadillo-Hinojosa, F., Félix-Bermúdez, A., Torres-Delgado, E.V., Durazo, R., Camacho-Ibar, V., Mejía, A., et al. 2020. Impacts of the 2014-2015 warm-water anomalies on nutrients, chlorophyll-*a* and hydrographic conditions in the coastal zone of northern Baja California. Journal of Geophysical Research, 125. doi: 10.1029/2020JC016473

Dirección General Marítima-Centro de Investigaciones Oceanográficas e Hidrográficas del Caribe (Dimar-CIOH). 2011. Catálogo de fitoplancton de la Bahía de Cartagena, Bahía Portete y Agua de Lastre. Serie de Publicaciones Especiales CIOH Vol. 5. Dimar, Cartagena de Indias.

Durazo, R. 2015. Seasonality of the transitional region of the California Current System off Baja California. Journal of Geophysical Research, 120: 1173-1196. doi: 10.1002/2014JC010405

Espinosa-Carreón, T.L., Gaxiola-Castro, G., Robles-Pacheco, J.M. & Nájera-Martínez, S. 2001. Temperatura, salinidad, nutrientes y clorofila a en aguas costeras de la Ensenada Sur de California. Ciencias Marinas, 27: 397-422.

Falkowski, P.G. & Raven, J.V. 1997. Aquatic photosynthesis. Blackwell Science, Massachusetts.

Fimbres-Martínez, M. 2019. Distribución y abundancia de microalgas ictiotóxicas en la costa noroeste de Baja California, México. M.Sc. Thesis, CICESE, Ensenada.

Finkel, Z.V., Beardall, J., Flynn, K., Quigg, A., Rees, T.A.V. & Raven, J.A. 2010. Phytoplankton in a changing world: cell size and elemental stoichiometry. Journal of Plankton Research, 32: 19-137. doi: 10.1093/plankt/fbp098

Flores-Vidal, X., González-Montes, S., Zertuche-Chanes, R., Rodríguez-Padilla, I., Marti, C.L., Imberger, J., et al. 2018. Three-dimensional exchange flows in a semi-enclosed bay: numerical simulations and high frequency radar observations. Estuarine Coastal and Shelf Science, 210: 26-35. doi: 10.1016/j.ecss.2018.05.027

García-Mendoza, E., Rivas, D., Olivos-Ortiz, A., Almazán-Becerril, A., Castañeda-Vega, C. & Peña-Manjarrez, J.L. 2009. A toxic *Pseudo-nitzschia* bloom in Todos Santos Bay, Northwestern Baja California, México. Harmful Algae, 8: 493-503. doi: 10.1016/j.hal.2008.10.002

Góngora-González, D.T. 2003. Estudio taxonómico de Peridiniales (Dinophycea): relación entre los estadios quísticos y vegetativo. Tesis de Grado, Centro de Investigaciones Biológicas del Noroeste, S.C., La Paz.

González-Silvera, A., Santamaría-del-Ángel, E., Camacho-Ibar, V., López-Calderón, J., Santander-Cruz, J. & Mercado-Santana, A. 2020. The effect of cold and warm anomalies on phytoplankton pigment composition in waters off the northern Baja California Peninsula (México): 2007-2016. Journal of Marine Science and Engineering, 8: 533. doi: 10.3390/jmse8070533

Guiry, M.D. & Guiry, G.M. 2022. AlgaeBase. Worldwide electronic publication, National University of Ireland, Galway. [https://www.algaebase.org]. Reviewed: March 20, 2022.

Higgins, H.W., Wright, SW. & Schlüter, L. 2011. Quantitative interpretation of chemotaxonomic pigment data. In: Roy, S., Llewellyn, C.A., Egeland, S.A. & Johnsen, G. (Eds.). Phytoplankton pigments: characterization, chemotaxonomy and applications in oceanography. Cambridge University Press, London, pp. 257-313.

Hooker S.B., Van Heukelem L., Thomas C.S., Claustre, H., Ras, J., Schluter, L., et al 2009. The third Sea-WiFS HPLC analysis Round-Robin experiment (SeaHARRE-2). National Aeronautics and Space Administration Goddard Space Flight Center, Greenbelt.

Jeffrey, S.W., Mantoura, R.F.C. & Wright, S.W. 1997. Phytoplankton pigments in oceanography: guidelines and modern methods. UNESCO Publishing, Paris.

Jeffrey S.W., Writght S.W. & Zapata M. 2011. Microalgal classes and their signature pigments. In: Roy, S., Llewellyn, C.A., Egeland, S.A. & Johnsen, G. (Eds.). Phytoplankton pigments: characterization, chemotaxonomy and applications in oceanography. Cambridge University Press, London, pp. 3-77.

Jim-Jeong, H.J., Du-Yoo, Y., Yeon-Park, J., Yoon-Song, J., Taek-Kim, S., Hyun-Lee, S., et al. 2005. Feeding by phytoplankton red-tide dinoflagellates: five species newly revealed and six species previously known to be mixotrophic. Aquatic Microbial Ecology, 40: 133-150. doi: 10.3354/ame040133

Jiménez-Herrera, H. 2017. Cambios en la estructura de la comunidad fitoplanctónica de la Bahía de Todos Santos durante la época de agosto 2014 a diciembre de 2015. Ensenada, Baja California, México. Bachelor Thesis, Universidad Autónoma de Baja California, Ensenada.

Kahru, M., Di Lorenzo, E., Manzano-Sarabia, M. & Mitchell, B.G. 2012. Spatial and temporal statistics of sea surface temperature and chlorophyll fronts in the California Current. Journal of Plankton Research, 34: 749-760. doi: 10.1093/plankt/fbs010

Kahru, M., Kudela, R.M., Anderson, C.R. & Mitchell, B.G. 2015. Optimized merger of ocean chlorophyll algorithms of MODIS-Aqua and VIIRS. IEEE Transactions on Geoscience and Remote Sensing, 12: 2282-2285. doi: 10.1109/LGRS.2015.2470250

Linacre, L., Landry, M.R., Cajal-Medrano, R., Lara-Lara, J.R., Hernández-Ayón, J.M., Mouriño-Pérez, R.R., et al. 2012. Temporal dynamics of carbon flow through the microbial plankton community in a coastal upwelling system off northern Baja California, Mexico. Marine Ecology Progress Series, 461: 31-46. doi: 10.3354/meps09782

Mackey, M.D., Mackey, D.J., Higgins, W.H. & Wright, S.W. 1996. CHEMTAX - a program for estimating class abundances from chemical markers: application to HPLC measurements of phytoplankton. Marine Ecology Progress Series, 144: 265-283. doi: 10.3354/meps144265

Martínez-Gaxiola, M.D., Peña-Manjarrez, J.L., Gaxiola-Castro, G., de la Cruz-Orozco, M.E. & García-Córdova, J. 2007. Flujo de CO_2 océano-atmósfera en Bahía de Todos Santos, Baja California, durante un florecimiento algal. In: Hernández-de-la-Torre, B. & Gaxiola-Castro, G. (Eds.). Carbono en ecosistemas acuáticos de México. Secretaría de Medio Ambiente y Recursos Naturales, INE-CICESE, Ensenada.

Mateos, E., Marinone, S.G. & Parés-Sierra, A. 2009. Towards the numerical simulation of the summer circulation in Todos Santos Bay, Ensenada, B.C., México. Ocean Modelling, 27: 107-112. doi: 10.1016/j.ocemod.2008.11.002

Meave del Castillo, M.E. 1999. Diatomeas planctónicas del Océano Pacífico de México. Informe final SNIB-CONABIO Proyecto N°H176. Universidad Autónoma Metropolitana, Unidad Iztapalapa, México D.F.

Medina-Elizalde, J., García-Mendoza, E., Ruiz-de la Torre, M.C., Peña-Manjarrez, J.L., Sánchez-Bravo, Y.A. & Paredes-Banda, P.E. 2016. Florecimientos algales nocivos y su impacto ecológico, económico y a la salud pública en la costa occidental de la península de Baja California. In: García-Mendoza, E., Quijano-Scheggia, I., Olivos-Ortiz, A. & Núñez-Vázquez, E.J. (Eds.). Florecimientos algales nocivos en México. CICESE, Ensenada.

Morales-Pulido, J.M. & Aké-Castillo, J.A. 2019. *Coscinodiscus* y *Coscinodiscopsis* (Bacillariophyceae) del Parque Nacional Sistema Arrecifal Veracruzano, Golfo de México. Revista Mexicana de Biodiversidad, 90: e902790. doi: 10.22201/ib.20078706e.2019.90.2790

Mouw, C.B., Barnett, A., McKinley, G.A., Gloege, L. & Pilcher, D. 2016. Phytoplankton size impact on export flux in the global ocean. Global Biogeochemical Cycles, 30: 1542-1562. doi: 10.1002/2015GB005355

Oliva-Méndez, N., Delgadillo-Hinojosa, F., Pérez-Brunius, P., Valencia-Gasti, A., Huerta-Díaz, M.A., Palacios-Coria, E. & Hernández-Ayón, J.M. 2018. The carbonate system in coastal waters off the northern region of the Baja California Peninsula under La Niña conditions. Ciencias Marinas, 44: 203-220. doi: 10.7773/cm.v44i3.2833

Orellana-Cepeda, E., Granados-Machuca, C. & Serrano-Esquer, J. 2004. *Ceratium furca*: one possible cause of mass mortality of cultured blue-fin Tuna at Baja California, México. In: Steidinger, K.A., Landsberg, J.H., Tomas, C.R. & Vargo, G.A. (Eds.). Harmful algae 2002. Florida Fish and Wildlife Conservation Commission, Florida Institute of Oceanography and Intergovernmental Oceanographic Commission of UNESCO, Florida, pp. 514-516.

Peña-Manjarrez, J.L., Gaxiola-Castro, G. & Helenes-Escamilla, J. 2009. Environmental factors influencing the variability of *Lingulodinium polyedra* and *Scrippsiella trochoidea* (Dinophyceae) cyst production. Ciencias Marinas, 35: 1-14. doi: 10.7773/cm.v35i1.1406

Peña-Manjarrez, J.L., Helenes, J., Gaxiola-Castro, G. & Orellana-Cepeda, E. 2005. Dinoflagellate cysts and bloom events at Todos Santos Bay, Baja California, México, 1999-2000. Continental Shelf Research, 25: 1375-1393. doi: 10.1016/j.csr.2005.02.002

Smalley, GW. & Coats, D.W. 2002. Ecology of the red tide dinoflagellate *Ceratium furca*: distribution, mixotrophy and grazing impact on ciliate populations of Chesapeake Bay. Journal of Eukaryotic Microbiology, 49: 63-73. doi: 10.1111/j.1550-7408.2002.tb00343.x

Stoecker, D.K., Hansen, P.J., Caron, D.A. & Mitra, A. 2017. Mixotrophy in the marine plankton. Annual Review of Marine Science, 9: 311-335. doi: 10.1146/annurev-marine-010816-060617

Tanahara, S., Canino-Herrera, S.R., Durazo, R., Félix-Bermúdez, A., Vivanco-Aranda, M., Morales-Estrada, E. & Lugo-Ibarra, K.C. 2021. Spatial and temporal variations in water quality of Todos Santos Bay, northwestern Baja California, Mexico. Marine Pollution Bulletin, 173: 113148. doi: 10.1016/j.marpolbul.2021.113148

Tester, P.A., Geesey, M.E., Guo, C., Paerl, H.W. & Millie, D.F. 1995. Evaluating phytoplankton dynamics in the Newport River estuary (North Carolina, USA) by HPLC-derived pigment profiles. Marine Ecology Progress Series, 124: 237-245.

Tomas, C. 1997. Identifying marine phytoplankton. Academic Press, New York.

Thomas, C. 2012. The HPLC method. In: Hooker, S.B., Clementson, L. & Thomas, C.S. (Eds.). The Fifth SeaWiFs HPLC analysis round-robin experiment (SeaHARRE-5). NASA Technical Memorandum, Houston, pp. 63-72.

Throndsen, J. 1978. Preservation and storage. In: Sournia, A. (Ed.). Phytoplankton manual. Monographs on Oceanographic Methodology. UNESCO, Paris.

Throndsen, J. 1993. The planktonic marine flagellates. In: Tomas, C.R. (Ed.). Marine phytoplankton: a guide to naked flagellates and coccolithophorids. Academic Press, New York, pp. 7-145.

Utermöhl, H. 1958. Vervollkmmung der quentitativen Phytoplankton-Methodik. Mitteilungen der International Vereinigung fur heorestische und Angewandted Limnologie, 1: 1-38.

Van-Heukelem, L. & Thomas, C.S. 2001. Computer-assisted high-performance liquid chromatography method development with applications to the isolation and analysis of phytoplankton pigments. Journal of Chromatography, 910: 31-49. doi: 10.1016/S0378-4347(00)00603-4

Wright, S.W. 1996. Analysis of phytoplankton of the Australian sector of the Southern Ocean: composition of microscopy and size frequency data with interpretations of pigment HPLC data using the CHEMTAX matrix factorization program. Marine Ecology Progress Series, 144: 285-29.

Wright, S.W., Ishikawa, A., Marchant, H.J., Davidson, A.T., Van den Enden, R.L. & Nash, G.V. 2009. Composition and significance of picophytoplankton in Antarctic waters. Polar Biology, 32: 797-808. doi: 10.1007/s0030 0-009-0582-9

Received: September 15, 2022; Accepted: November 3, 2022

Table S1. Output ratios of pigment markers by sampling day. Pigment abbreviations are indicated in Table 1.

a) February 2017									
Grup/Pigment	Chl-*b*	19´-But	19´-Hex	Allo	Fuco	Peri	Zea	Lut	Chl c_3
Diatoms	0	0	0	0	0.41	0	0	0	0
Dinoflagellates	0	0	0	0	0	0.5	0	0	0
Prymnesiophytes	0	0.03	0.26	0	0.12	0	0	0	0.13
Chlorophytes	0.31	0	0	0	0	0	0.02	0.02	0
Cryptophytes	0	0	0	0.35	0	0	0	0	0
Chrysophytes	0	0	0	0	0	0	0.36	0	0
Cyanobacteria	0	0.20	0	0	0	0	0	0	0.44
b) March 2017									
Grup/Pigment	Chl-*b*	19´-But	19´-Hex	Allo	Fuco	Peri	Zea	Lut	Chl c_3
Diatoms	0	0	0	0	0.407	0	0	0	0
Dinoflagellates	0	0	0	0	0	0.516	0	0	0
Prymnesiophytes	0	0.03	0.27	0	0.107	0	0	0	0.141
Chlorophytes	0.29	0	0	0	0	0	0.018	0.018	0
Cryptophytes	0	0	0	0.30	0	0	0	0	0
Chrysophytes	0	0	0	0	0	0	0.375	0	0
Cyanobacteria	0	0.19	0	0	0	0	0	0	0.457
c) June 2017									
Grup/Pigment	Chl-*b*	19´-But	19´-Hex	Allo	Fuco	Peri	Zea	Lut	Chl c_3
Diatoms	0	0	0	0	0.427	0	0	0	0
Dinoflagellates	0	0	0	0	0	0.533	0	0	0
Prymnesiophytes	0	0.029	0.235	0	0.125	0	0	0	0.165
Chlorophytes	0.283	0	0	0	0	0	0.021	0.018	0
Cryptophytes	0	0	0	0.293	0	0	0	0	0
Chrysophytes	0	0	0	0	0	0	0.359	0	0
Cyanobacteria	0	0.295	0	0	0	0	0	0	0.096
d) November 2017									
Grup/Pigment	Chl-*b*	19´-But	19´-Hex	Allo	Fuco	Peri	Zea	Lut	Chl c_3
Diatoms	0	0	0	0	0.390	0	0	0	0
Dinoflagellates	0	0	0	0	0	0.511	0	0	0
Prymnesiophytes	0	0.026	0.267	0	0.122	0	0	0	0.136
Chlorophytes	0.296	0	0	0	0	0	0.017	0.018	0
Cryptophytes	0	0	0	0.290	0	0	0	0	0
Chrysophytes	0	0	0	0	0	0	0.409	0	0
Cyanobacteria	0	0.164	0	0	0	0	0	0	0.457
e) February 2018									
Grup/Pigment	Chl-*b*	19´-But	19´-Hex	Allo	Fuco	Peri	Zea	Lut	Chl c_3
Diatoms	0	0	0	0	0.416	0	0	0	0
Dinoflagellates	0	0	0	0	0	0.544	0	0	0
Prymnesiophytes	0	0.029	0.282	0	0.132	0	0	0	0.121
Chlorophytes	0.279	0	0	0	0	0	0.019	0.021	0
Cryptophytes	0	0	0	0.261	0	0	0	0	0
Chrysophytes	0	0	0	0	0	0	0.383	0	0
Cyanobacteria	0	0.091	0	0	0	0	0	0	0.614
f) June 2018									
Grup/Pigment	Chl-*b*	19´-But	19´-Hex	Allo	Fuco	Peri	Zea	Lut	Chl c_3
Diatoms	0	0	0	0	0.406	0	0	0	0
Dinoflagellates	0	0	0	0	0	0.506	0	0	0
Prymnesiophytes	0	0.028	0.288	0	0.109	0	0	0	0.138
Chlorophytes	0.281	0	0	0	0	0	0.018	0.021	0
Cryptophytes	0	0	0	**0.330**	0	0	0	0	0
Chrysophytes	0	0	0	0	0	0	0.390	0	0
Cyanobacteria	0	0.132	0	0	0	0	0	0	0.544

Continuation

g) August 2018									
Grup/Pigment	Chl-*b*	19´-But	19´-Hex	Allo	Fuco	Peri	Zea	Lut	Chl c_3
Diatoms	0	0	0	0	0.391	0	0	0	0
Dinoflagellates	0	0	0	0	0	0.520	0	0	0
Prymnesiophytes	0	0.028	0.294	0	0.123	0	0	0	0.114
Chlorophytes	0.282	0	0	0	0	0	0.019	0.020	0
Cryptophytes	0	0	0	0.314	0	0	0	0	0
Chrysophytes	0	0	0	0	0	0	0.368	0	0
Cyanobacteria	0	0.067	0	0	0	0	0	0	0.727
h) October 2018									
Grup/Pigment	Chl-*b*	19´-But	19´-Hex	Allo	Fuco	Peri	Zea	Lut	Chl c_3
Diatoms	0	0	0	0	0.391	0	0	0	0
Dinoflagellates	0	0	0	0	0	0.510	0	0	0
Prymnesiophytes	0	0.028	0.271	0	0.125	0	0	0	0.115
Chlorophytes	0.293	0	0	0	0	0	0.017	0.018	0
Cryptophytes	0	0	0	0.327	0	0	0	0	0
Chrysophytes	0	0	0	0	0	0	0.384	0	0
Cyanobacteria	0	0.099	0	0	0	0	0	0	0.643

Table S2. List of presence/absence of genera and species observed in the study region by date and station. Those in bold letters are the most frequent or abundant.

Genus/Species	Feb-17						Mar-17						Jun-17						Nov-17						Feb-18						Jun-18						Ago-18						Oct-18					
	1	2	3	4	5	6	1	2	3	4	5	6	1	2	3	4	5	6	1	2	3	4	5	6	1	2	3	4	5	6	1	2	3	4	5	6	1	2	3	4	5	6	1	2	3	4	5	6
Dinophyta																																															
Alexandrium acatenella													X																																			
Alexandrium sp.																								X																							
Blepharocysta sp.																																					X										
Centrodinium sp.																	X	X																												
Ceratoperidinium sp.																												X																		
Cochlodinium sp.		X		X	X	X																									**X**	**X**	**X**	**X**	**X**	**X**	**X**	**X**	**X**	**X**	**X**	**X**	**X**	**X**		**X**	**X**	**X**
Dinophysis acuminata		X																														X														
Dinophysis caudata		X					X			X		X											X						X														X			
Dinophysis sp.							X					X					X	X							X		X		X	X		X		X	X									X		
Dinophysis tripos																								X								X														
Gymnodinium sp.							X			X			X	X		X		X						X						X	X	X		X	X	X		X			X			X	X	X
Gyrodinium sp.					X													X					X			X	X	X		X						X	X	X	X	X	X			X	X	X
Heterocapsa sp.																																												X				
Lingulodinium polyedra		**X**					**X**			**X**		**X**	**X**	**X**	**X**	**X**	**X**	**X**					**X**	**X**	**X**	**X**	**X**	**X**	**X**	**X**	**X**	**X**	**X**	**X**	**X**	**X**	**X**	**X**					**X**			**X**
Ornithocercus sp.															X															X																	
Oxytoxum laticeps																																			X												
Oxytoxum scolopax		X	X	X	X								X	X		X	X	X						X						X																	
Oxytoxum sp.																											X			X	X	X	X	X	X	X	X	X		X	X	X	X		X	X	X	X		X
Podolampas palmipes																																		X														
Podolampas sp.																											X									X							X	X				
Polykrikos kofoidii																																		X														
Prorocentrum arcuatum							X							X		X	X							X																							
Prorocentrum gracile		**X**	**X**	**X**	**X**	**X**	**X**			**X**		**X**	**X**	**X**		**X**	**X**	**X**		**X**	**X**	**X**	**X**	**X**	**X**		**X**	**X**	**X**	**X**	**X**	**X**	**X**	**X**	**X**	**X**	**X**	**X**	**X**	**X**	**X**	**X**	**X**	**X**	**X**	**X**	**X**	**X**	**X**
Prorocentrum lima																						X																										
Prorocentrum micans		**X**	**X**				**X**					**X**	**X**		**X**	**X**	**X**	**X**							**X**	**X**	**X**	**X**	**X**	**X**	**X**	**X**	**X**	**X**	**X**	**X**	**X**	**X**			**X**							**X**
Prorocentrum sp.																																X						X			X	X	X	X		X			
Protoperidinium sp.			**X**	**X**	**X**	**X**	**X**	**X**		**X**		**X**	**X**	**X**			**X**	**X**		**X**	**X**	**X**	**X**				**X**	**X**	**X**	**X**	**X**	**X**	**X**	**X**	**X**	**X**	**X**	**X**	**X**	**X**	**X**	**X**	**X**	**X**	**X**	**X**			
Protoperidinium divergens																													X	X	X	X	X	X														
Pyrophacus sp.																																X				X			X			X			X	X		
Scrippsiella sp.		X	X	X	X	X																									X	X	X	X	X	X	X	X	X	X	X	X	X	X	X	X	X	X
Torodinium robustum																																	X		X													
Torodinium sp.																															X		X							X				X				
Tripos candelabrum																																			X													
Ceratium tripos var. divaricatum		X	X			X																					X					X			X	X	X										
Ceratium falcatum												X																									X	X				X	X						
Tripos furca		**X**	**X**	**X**	**X**	**X**							**X**				**X**				**X**		**X**	**X**	**X**		**X**	**X**	**X**		**X**	**X**		**X**	**X**	**X**			**X**			**X**	**X**	**X**	**X**			
Tripos fusus			**X**		**X**		**X**					**X**	**X**	**X**		**X**	**X**	**X**				**X**		**X**	**X**	**X**		**X**	**X**	**X**		**X**	**X**		**X**	**X**	**X**	**X**	**X**			**X**	**X**	**X**	**X**			
Tripos hircus							X			X		X	X		X	X							X																								
Ceratium tripos var. macroceros																																	X														
Tripos sp.										X			X												X				X																		
Tripos spp.1																																																
Tripos spp.2																																																
Ceratium tripos var. breve										X									X																													

Continuation

Genus/Species	Feb-17						Mar-17						Jun-17						Nov-17						Feb-18						Jun-18						Ago-18						Oct-18					
	1	2	3	4	5	6	1	2	3	4	5	6	1	2	3	4	5	6	1	2	3	4	5	6	1	2	3	4	5	6	1	2	3	4	5	6	1	2	3	4	5	6	1	2	3	4	5	6
Bacillariophyta																																															
Amphora sp.																				X	X																											
Asterionellopsis glacialis													X																																		
Asteromphalus sp.					X														X		X			X							X						X				X		X			
Bacteriastrum furcatum																							X	X								X					X		X	X						
Bacteriastrum sp.				X												X	X	X									X	X	X	X				X									X				
Bacteriastrum spp. 1																							X	X																							
Bacteriastrum spp.2							X								X																															
Biddulphia sp.																										X																				
Chaetoceros decipiens																						X	X								X	X	X	X	X								X	X	X		
Chaetoceros densus																															X	X														
Chaetoceros didymus																																	X	X												
Chaetoceros lorenzianus																						X											X	X	X											X
Chaetoceros messanensis																																		X												
Chaetoceros peruvianus																															X	X	X	X	X										X	
Chaetoceros pseudocurvisetus																												X																		
Chaetoceros sp.				X																				X	X	X	X	X	X	X	X	X			X	X	X	X	X	X	X	X	X			X	X
Chaetoceros spp. 1			X																																											
Chaetoceros spp. 2													X		X		X																														
Chaetoceros spp.3																			X			X																								
Coscinodiscus granii																								X										X												
Coscinodiscus perforatus																								X										X												
Coscinodiscus sp.										X				X		X		X		X	X	X	X	X			X	X		X	X			X	X								X				
Coscinodiscus spp. 1							X																																								
Coscinodiscus spp.2																			X																												
Cylindrotheca closterium														**X**			**X**			**X**			**X**	**X**	**X**	**X**	**X**	**X**	**X**	**X**	**X**	**X**	**X**			**X**	**X**	**X**	**X**	**X**	**X**	**X**	**X**	**X**	**X**	**X**	**X**	**X**	**X**
Cymbella sp.																												X																		
Diploneis sp.																																					X										
Eucampia sp.																			X		X					X	X			X			X				X	X		X							
Fragilaria sp.															X														X																		
Grammatophora marina																																															
Guinardia sp.																												X	X	X																	
Guinardia striata													**X**			**X**	**X**		**X**	**X**	**X**	**X**	**X**	**X**	**X**	**X**	**X**				**X**	**X**	**X**	**X**	**X**	**X**	**X**	**X**	**X**	**X**	**X**	**X**	**X**	**X**	**X**	**X**	**X**	**X**
Hemiaulus hauckii																	**X**									**X**								**X**				**X**	**X**	**X**	**X**	**X**	**X**	**X**	**X**	**X**	**X**	**X**	**X**
Hemiaulus sinensis																									X									X												
Hemiaulus sp.																	X					X																								
Leptocylindrus sp.																X									X	X		X	X	X	X	X	X	X	X											
Licmophora ehrenbergii																						X	X											X	X											
Lyrella sp.														X					X																												
Melossira sp.														X										X	X			X	X	X							X						X				
Navicula delicatula															X	X						X		X	X	X																				
Navicula directa														X			X							X																						
Navicula distans																X	X	X				X																								
Navicula marina													X							X	X	X	X		X	X	X	X	X		X	X	X	X	X								X	X	X	X	X	X
Navicula sp.							X						X	X		X								X	X			X			X	X	X	X	X	X	X	X	X			X				
Navicula spp. 1																																															
Navicula spp.2																		X																													
Nitzschia longissima													X	X		X	X						X	X		X								X												
Nitzschia sp.																X	X			X	X				X			X			X	X	X	X			X	X			X	X		X		
Noctiluca sp.										X					X		X									X	X	X	X	X																
Odontella sinensis																						X	X	X	X												X									
Planktoniella sol													X				X							X																						
Pseudo-nitzschia fraudulenta																														X																
Pseudo-nitzschia sp.							**X**						**X**	**X**			**X**		**X**	**X**	**X**	**X**	**X**	**X**	**X**	**X**	**X**	**X**	**X**	**X**	**X**	**X**	**X**	**X**	**X**		**X**	**X**	**X**		**X**	**X**	**X**		**X**		**X**	**X**
Pleurosigma sp.															X	X										X			X	X																
Rhabdonema sp.																									X																					
Rhizosolenia imbricata							X													X			X	X								X	X									X		X			X
Rhizosolenia pungens							X										X								X	X		X				X	X				X									
Rhizosolenia setigera																										X					X															
Rhizosolenia sp.													X						X		X	X										**X**	**X**	**X**	**X**	**X**	**X**	**X**	**X**	**X**		**X**		**X**	**X**	**X**
Rhizosolenia styliformis																				X		X			X	X	X		X		X			X											
Skeletonema costatum																			X					X										X			X	X			X					
Thalassionema nitzschioides					X	X									X						X				X	X	X	X	X	X	X	X	X	X	X										
Thalassiosira rotula																								X																						
Thalassiosira sp.																	X		X																											

Continuation

Genus/Species	Feb-17						Mar-17						Jun-17						Nov-17						Feb-18						Jun-18						Ago-18						Oct-18					
	1	2	3	4	5	6	1	2	3	4	5	6	1	2	3	4	5	6	1	2	3	4	5	6	1	2	3	4	5	6	1	2	3	4	5	6	1	2	3	4	5	6	1	2	3	4	5	6
Chrysophyta																																															
Dictyocha calida																					X																										
Dictyocha fibula																			X				X	X																			X	X	X	X		
Dictyocha sp.				X			X								X	X									X	X	X	X	X	X	X	X			X	X	X	X	X	X	X	X						
Chlorophyta																																															
Pyraminmonas grossii																																												X					
Prymnesiophyta																																															
Phaeocystis sp.													X							X											X			X	X	X							X	X	X	X	X	X
Phaeocystis globosa						X																											X				X	X						X					
Raphydophyta																																															
Chatonella marina						X																									X		X					X	X	X	X	X						
Fibrocapsa sp.																			X																								X	X				
Euglenophyta																																															
Euglena sp.																						X																								
Eutreptia sp.																																														X	
Cryptophyta																																															
Leucocryptos marina																															X		X											X	X		X		
Teleaulax acuta																							X																					X				